larger databases are developed, the need for the invasive procedures may lessen.

Ann Jakubowski
David A. Scheinberg
Leukemia and Clinical Immunology Services
Memorial Sloan-Kettering Cancer Center
New York, New York

REFERENCES

1. Chung JK, Yeo J, Lee DS, et al. Bone marrow immunoscintigraphy using ^{99m}Tc-labeled antigranulocyte antibody in hematologic disorders. *J Nucl Med* 1996;37:948–952.
2. Vogler JB, Murphy WA. Bone marrow imaging. *Radiology* 1988;168:679–693.
3. Negendank W, Weisman D, Bey TM, et al. Evidence for clonal disease by magnetic resonance imaging in patients with hypoplastic marrow disorders. *Blood* 1991;78:2872–2879.
4. Agris PF, Campbell ID. Proton nuclear magnetic resonance of intact friend leukemia cells; phosphorylcholine increase during differentiation. *Science* 1982; 216:1325–1327.
5. Jensen KE, Jensen M, Grundtvig P, et al. Localized in vivo proton spectroscopy of the bone marrow in patients with leukemia. *Magnetic Resonance Imaging* 1990;8:779–789.
6. Larson SM, Nelp WB. The radiocolloid bone marrow scan in malignant disease. *J Surg Oncol* 1971;3:685–697.
7. Choi CW, Chung JK, Lee DS, et al. Development of bone marrow immunoscintigraphy using a ^{99m}Tc-labeled anti-NCA-95 monoclonal antibody. *Nucl Med Biol* 1995;22:117–123.
8. Appelbaum FR, Matthews DC, Eary JF, et al. The use of radiolabeled anti-CD33 antibody to augment marrow irradiation prior to marrow transplantation for acute myelogenous leukemia. *Transplantation* 1992; 54:829.
9. Caron PC, Jurcic JG, Scott AM, et al. A Phase 1B trial of humanized monoclonal antibody M195 (Anti-CD33) in myeloid leukemia: specific targeting without immunogenicity. *Blood* 1994;7:1760–1768.
10. Sgouros G, Graham MC, Divgi CR, et al. Modeling and dosimetry of monoclonal antibody M195 (Anti-CD33) in acute myelogenous leukemia. *J Nucl Med* 1993;34:422–430.
11. Jurcic JG, Caron PC, Miller WH Jr, et al. Sequential targeted therapy for relapsed acute promyelocytic leukemia with all-*trans* retinoic acid and anti-CD33 monoclonal antibody M195. *Leukemia* 1995;9:244–248.
12. Schwartz MA, Lovett DR, Redner A, et al. Dose escalation trial of ^{131}I-M195 (Anti-CD33) for cytoreduction and marrow ablation in relapsed or refractory myeloid leukemias. *J Clin Oncol* 1993; 11:294–303.
13. Glaspy JA, Hawkins R, Hoh CK, et al. Use of positron emission tomography in oncology. *Oncology* 1993;7: 41–50.
14. Larson SM. Positron emission tomography in oncology and allied diseases. In: Devita VT, Hellman S, Rosenberg SA, eds. *Cancer, principles and practice of oncology*, 2nd ed. Philadelphia: JB Lippincott; 1989: 1–12.
15. Dahlbom M, Hoffman EJ, Hoh CK, et al. Evaluation of a positron emission tomography scanner for whole-body imaging. *J Nucl Med* 1992;33:1191–1199.

FDG-PET to Evaluate Response to Hyperthermic Isolated Limb Perfusion for Locally Advanced Soft-Tissue Sarcoma

Robert J. van Ginkel, Harald J. Hoekstra, Jan Pruim, Omgo E. Nieweg, Willemina M. Molenaar, Anne M.J. Paans, Antoon T.M. Willemsen, Willem Vaalburg and Heimen Schraffordt Koops
Department of Surgical Oncology, PET Center and Department of Pathology, University Hospital Groningen, The Netherlands; and Department of Surgery, The Netherlands Cancer Institute, Amsterdam, The Netherlands

We investigated FDG-PET in patients undergoing hyperthermic isolated limb perfusion (HILP) with rTNF-α, rIFN-γ and melphalan for locally advanced soft-tissue sarcoma of the extremities. **Methods:** Twenty patients (11 women, 9 men; aged 18–80 yr, mean age 49 yr) were studied. FDG-PET studies were performed before, 2 and 8 wk after HILP. After the final PET study, the tumor was resected and pathologically graded. Patients with pathologically complete response (pCR) showed no viable tumor after treatment. Those with pathologically partial response (pPR) showed various amounts of viable tumor in the resected specimens. **Results:** Seven patients showed a pCR (35%) and 12 patients showed a pPR (60%). In one patient, pathological examination was not performed (5%). The pre-perfusion glucose consumption in the pCR group was significantly higher than in the pPR group ($p < 0.05$). Visual analysis of the PET images after perfusion showed a rim of increased FDG uptake around a core of absent FDG uptake in 12 patients. The rim signal contained a fibrous pseudocapsule with inflammatory tissue in the pCR group, viable tumor was seen in the pPR group. The glucose consumption in the pCR group at 2 and 8 wk after perfusion had decreased significantly ($p < 0.05$) in comparison to the glucose consumption in the pPR. **Conclusion:** Based on the pretreatment glucose consumption in soft-tissue sarcomas, one could predict the probability of a patient achieving complete pathological response after HILP. FDG-PET indicated the pathologic tumor response to HILP, although the lack of specificity of FDG, in terms of differentiation between an inflammatory response and viable tumor tissue, hampered the discrimination between pCR and pPR.

Received May 22, 1995; revision accepted Nov. 7, 1995.

For correspondence or reprints contact: Harald J. Hoekstra, MD, PhD, Division of Surgical Oncology, Department of Surgery, Groningen University Hospital, PO Box 30.001, 9700 RB Groningen, The Netherlands.

Key Words: fluorine-18-fluorodeoxyglucose; PET; hyperthermic isolated limb perfusion; tumor necrosis factor; sarcoma

J Nucl Med 1996; 37:984–990

Malignant soft-tissue sarcomas are a heterogeneous group of lesions that all arise from tissue of mesenchymal origin and are characterized by aggressive local growth and hematogenic metastases. They account for 1% of all malignant tumors and have an incidence rate of 2 per 100,000. About 60% of these tumors occur in the extremities and are often quite large at diagnosis (*1*). Limb-saving treatment of extremity soft-tissue sarcomas is a multidisciplinary matter, with surgery and radiotherapy as the usual treatment protocol (*2,3*). This combination therapy has avoided ablative surgical procedures in the majority of patients.

The majority of locally advanced extremity soft-tissue sarcomas are treated by amputation. Intra-arterial chemotherapy with adriamycin, combined with preoperative radiotherapy, surgery and postoperative radiotherapy is effective in the treatment of locally advanced soft-tissue sarcoma, but significant morbidity does occur (*4*). Recently Eilber et al. (*5*) reported a complete response rate of 49% and a limb-saving rate of 98% with neo-adjuvant chemotherapy and radiation for high-grade extremity soft-tissue sarcoma with low-treatment morbidity. Hyperthermic isolated limb perfusion (HILP) also proved to be of value in the treatment for locally advanced extremity soft-tissue sarcoma (*6–8*). With HILP, chemotherapeutic tissue concentrations may be up to 20 times higher than can be attained with systemic administration (*9*). The intro-

TABLE 1
Tumor Characteristics for Each Patient

Patient no.	Histology		Grade	Number of lesions	Largest diameter (MRI)	Perfusion agents
1	Rhabdomyosarcoma	Primary	3	1	10 cm	TNF, IFN, Melphalan
2	Dedifferentiated myxoid liposarcoma	Primary	3	1	20 cm	TNF, IFN, Melphalan
3	Myxoid liposarcoma	Recurrent	1	2	15 cm	TNF, IFN, Melphalan
4	Peripheral neuroectodermal tumor	Primary	3	3	8 cm	TNF, Melphalan
5	Malignant fibrous histiocytoma	Primary	3	1	5 cm	TNF, Melphalan
6	Malignant fibrous histiocytoma	Recurrent	3	1	4 cm	TNF, Melphalan
7	Synovialsarcoma	Primary	3	1	8 cm	TNF, Melphalan
8	Myxoid chondrosarcoma	Primary	2	1	8 cm	TNF, IFN, Melphalan
9	Malignant fibrous histiocytoma	Primary	2	1	19 cm	TNF, IFN, Melphalan
10	Malignant fibrous histiocytoma	Recurrent	1	24*	2 cm	TNF, IFN, Melphalan
11	Malignant schwannoma	Recurrent	3	7	5 cm	TNF, Melphalan
12	Fibrosarcoma	Primary	3	1	23 cm	TNF, IFN, Melphalan
13	Synoviosarcoma	Primary	3	1	9 cm	TNF, IFN, Melphalan
14	Myxoid liposarcoma	Recurrent	1	2	8 cm	TNF, IFN, Melphalan
15	Dedifferentiated liposarcoma	Primary	2	1	17 cm	TNF, IFN, Melphalan
16	Leiomyosarcoma	Recurrent	3	1	12 cm	TNF, IFN, Melphalan
17	Angiosarcoma	Primary	3	1	30 cm	TNF, Melphalan
18	Malignant schwannoma	Recurrent	2	1	8 cm	TNF, IFN, Malphalan
19	Well-differentiated liposarcoma	Primary	1	1	29 cm	TNF, IFN, Melphalan
20	Malignant fibrous histiocytoma	Primary	3	4	5 cm	TNF, Melphalan

*Multiple small lesions of the lower leg (0.5–2 cm).
TNF = tumor necrosis factor; IFN = interferon.

duction of recombinant tumor necrosis factor-alpha (rTNF-α), interferon-gamma (rIFN-γ) and melphalan in regional perfusion represents a promising new development (*10*). With this perfusion regimen, a complete response rate of 55% and a partial response rate of 40% can be reached in the treatment of locally advanced soft-tissue sarcoma of the extremities with a limb-saving rate of 90% (*11*). Since 1991, this perfusion strategy has been used at our institution for these types of soft-tissue sarcomas.

PET enables visualization and quantification of metabolic processes in vivo. Fluorine-18-2-fluoro-2-deoxy-D-glucose (FDG) has proven to be of value in the visualization of various types of tumors (*12,13*). The use of FDG is based on Warburg's observation of increased glycolysis in cancer cells. The citric acid cycle, which is more efficient in adenosine tri-phosphate generation, is suppressed (*14*). As a result, cancer cells accumulate the glucose analog FDG which is trapped intracellularly as FDG phosphate. FDG-PET can visualize soft-tissue sarcomas, indicate the malignancy grade and detect locally recurrent disease (*15–17*). Various clinical reports suggest the feasibility of FDG-PET to assess tumor response to radiotherapy and chemotherapy (*18–20*). This particular application of PET as a noninvasive technique to evaluate the outcome of such often aggravating and expensive therapy may have a significant effect on patient management. Ineffective treatment could be adjusted or discontinued in an early stage and effective treatment could be continued with confidence. The perfusion protocol provides us with histology before and after regional chemotherapy. The tumor responses to this regional drug treatment are variable. This clinical setting creates an opportunity to investigate the value of a noninvasive diagnostic technique in the determination of tumor response to chemotherapy. The aim of the present study was to investigate FDG-PET in patients undergoing HILP for locally advanced soft-tissue sarcoma and to correlate PET findings with histology before and after treatment.

METHODS

Patients

Twenty (11 women, 9 men; aged 18–80 yr, mean age 49 yr) patients with biopsy proven soft-tissue sarcomas were entered in the study. Informed consent was obtained from each patient. The diagnosis of the tumors was determined in a standard fashion and graded according to Coindre (*21,22*). Thirteen patients presented with a newly diagnosed soft-tissue sarcoma (65%) and seven patients with a local recurrence (35%), that had been previously treated with surgery alone. Nineteen tumors were located in the lower limb (95%), and one patient (5%) had a sarcoma located in the right elbow. All tumors were considered primarily irresectable because of size, their multicentricity in the limb or fixation to the neurovascular bundle or bone. Median tumor size was 8.5 cm (range 2–30 cm). To render the tumors resectable for limb salvage, patients were treated with HILP.

Treatment Protocol

HILP is based on the technique developed by Creech and Krementz (*23*). Briefly, after ligation of all collateral vessels and heparinization of the patient with 3.3 mg heparin/kg bodyweight, the axillary, iliac, femoral or popliteal vessels were cannulated and connected to an extracorporeal circuit. The perfused limb was wrapped in a thermal blanket to reduce heat loss and a tourniquet was applied at the root of the extremity to minimize leakage of the perfusate into the systemic circulation. Perfusion was performed during 90 min under mild hyperthermia (39–40°C) and physiologically optimal conditions (*24*). At the start of perfusion, 3 mg (upper extremity) or 4 mg (lower extremity) rTNF-α were injected as a bolus into the arterial line. Melphalan was administered 30 min later, 10 mg/liter extremity volume (leg) or 13 mg/liter extremity volume (arm) (*25*). Since all perfusions were performed in a Phase II clinical trial, the initial 13 patients in the PET study also received a dose of 0.2 mg rINF-γ subcutaneously 1 and 2 days before perfusion, followed by 0.2 mg rINF-γ injected into the arterial line

TABLE 2
PET Results and Pathological Response for Each Patient

Patient no.	Visual evaluation of the PET studies: Before HILP (% of tumor active*)	Visual evaluation of the PET studies: After HILP (% of tumor active*)	Metabolic rate of glucose (μmole/100g/min): Before HILP: Tumor	2 wk after HILP: Tumor	2 wk after HILP: Rim	2 wk after HILP: Core	8 wk after HILP: Tumor	8 wk after HILP: Rim	8 wk after HILP: Core	Pathological evaluation: Response	% Viable tumor	Macro/ Microscopic view	Correspondence of PET with histology
1	100	<10	36.7	3.7	8.4	0.6	n.q.	n.q.	n.q.	pCR	0	Rim: pseudocapsule Core: necrosis	+
2	100	<10	41.8	n.p.	n.p.	n.p.	2.7	6.3	0.4	pCR	0	Rim: pseudocapsule Core: necrosis	+
3	80	80	3.6	n.q.	n.q.	n.q.	5.6	Absent	Absent	pCR	0	Regressive tumortissue	–
4	100	<10	33.2	6.2	7.9	1.8	5.4	7.2	1.5	pCR	0	Rim: pseudocapsule Core: necrosis	+
5	100	<10	36.3	5.0	6.5	1.4	4.3	6.1	0.9	pCR	0	Rim: pseudocapsule Core: necrosis	+
6	100	<10	13.3	12.8	Absent	Absent	0.9	Absent	Absent	pCR	0	Regressive tumortissue	+
7	100	<10	18.0	4.5	5.9	1.7	7.2	7.4	1.6	pCR	0	Rim: pseudocapsule Core: necrosis	+
8	50	50	6.4	4.6	6.3	1.2	3.9	5.2	0.9	pPR	<10	Rim: areas of viable tumor Core: necrosis	–
9	100	<10	13.0	4.4	9.1	0.5	4.8	7.4	0.3	pPR	<10	Rim: areas of viable tumor Core: necrosis	+
10	100	<10	4.8	7.0	Absent	Absent	n.p.	n.p.	n.p.	pPR	<10	Areas of viable tumor	+
11	100	<10	8.0	n.q.	n.q.	n.q.	5.9	Absent	Absent	pPR	<10	Areas of viable tumor	+
12	100	<10	n.q.	n.p.	n.p.	n.p.	5.8	9.0	1.5	pPR	<10	Rim: areas of viable tumor Core: necrosis	+
13	100	<10	12.5	5.0	8.1	1.2	3.6	6.9	1.0	pPR	<20	Rim: areas of viable tumor Core: necrosis	+
14	50	50	5.0	n.p.	n.p.	n.p.	4.2	Absent	Absent	pPR	50	Areas of viable tumor	+
15	50	50	12.5	9.0	Absent	Absent	10.0	Absent	Absent	pPR	50	Areas of viable tumor	+
16	50	50	22.5	5.7	10.1	1.0	n.p.	n.p.	n.p.	pPR	50	Rim: areas of viable tumor Core: necrosis	+
17	30	30	3.3	2.9	13.4	1.2	7.1	26.1	1.4	pPR	50	Rim: areas of viable tumor Core: necrosis	+
18	80	40	25.7	n.p.	n.p.	n.p.	11.3	17.3	2.4	pPR	50	Rim: areas of viable tumor Core: necrosis	+
19	100	100	4.3	5.8	Absent	Absent	4.3	Absent	Absent	pPR	100	Viable tumor	+
20	80	<20	24.2	4.4	8.4	3.0	n.p.	n.p.	n.p.	n.p.	n.p.	n.p.	n.p.

*Percentage of tumor volume active on PET study.
pCR = pathologically complete response; pPR = pathologically partial response; n.p. = not performed; n.q. = no quantification.

at the start of perfusion. The final seven patients in the PET study did not receive the rINF-γ. This alteration in treatment schedule was due to the decision of the trial commission to investigate the additional effect of rINF-γ in the perfusion regiment while the PET study was still in progress.

All perfusions were performed with a bubble oxygenator roller pump and heat exchanger. The perfusate was oxygenated by a mixture of O_2 and CO_2 and consisted of 350 ml 5% dextran 40 in glucose 5%, 500 ml blood (250 ml red blood cells, 250 ml plasma), 30 ml 8.4% $NaHCO_3$ and 0.5 ml 5000 IU/ml heparin. After 90 min of perfusion, the limb was flushed with 2 liters dextran 40 in glucose 5% and 500 ml blood (250 ml red blood cells, 250 ml plasma), catheters were removed, the circulation restored and the heparin antagonized with protamine chloride. A lateral fasciotomy

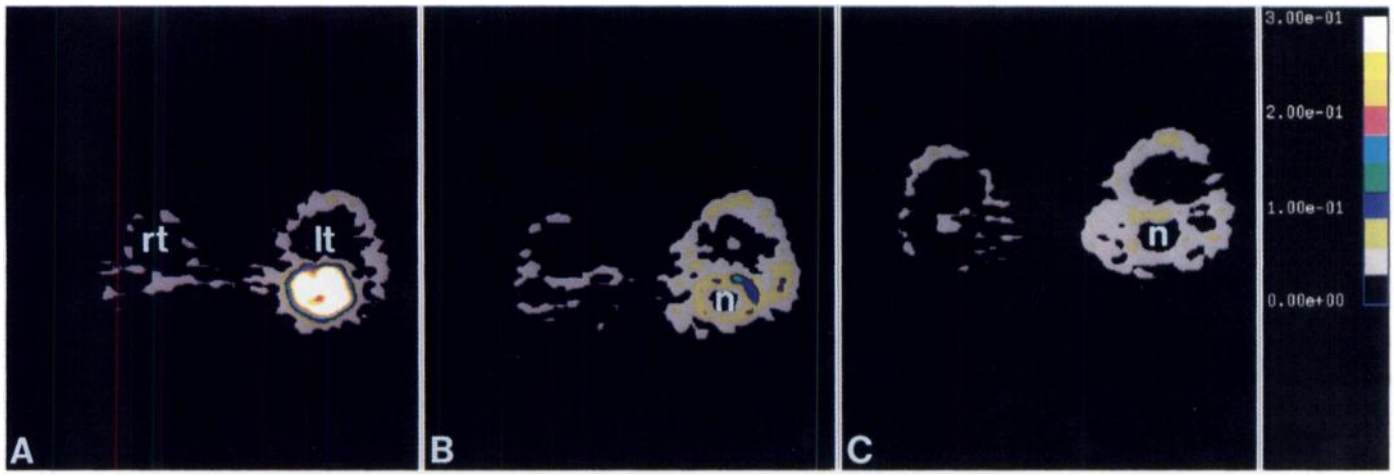

FIGURE 1. Transversal image of a malignant fibrous histiocytoma of the lower leg in Patient 5. Before perfusion (A), the tumor is clearly depicted as a homogeneous mass with glucose uptake of 36.3 μmole/100 g tissue/min. Two (B) and 8 wk after perfusion (C), the glucose uptake in the tumor decreased to 5.0 and 4.3, respectively. The center of the tumor became inactive surrounded by an active rim. Pathological examination revealed complete response. The rim signal corresponded with a fibrotic vascular pseudocapsule with inflammatory tissue surrounding a core of necrosis (n). The color scale equates a particular hue to a particular metabolic rate of glucose in mmol/100 g tissue/min (rt = right tibia; lt = left tibia).

of the anterior compartment of the lower leg or arm was performed to prevent compartment syndrome (*26*). Approximately 8 wk after perfusion (median 61 days, range 43–106 days), the residual tumor masses were excised and pathologically examined.

Pathological Examination

The tumor was measured in three dimensions and the percentage of necrosis estimated. Representative tumor sections were taken, encompassing macroscopically different tumor areas, including necrosis. Generally, one section per centimeter largest diameter with a minimum of three was taken. Based on an integration of gross and microscopic findings, a final estimate of the percentages of viable and necrotic or regressive tumor was made. If possible, macroscopic examination and tissue sampling were performed based on the latest PET images. The results were classified as either pathologically complete response (pCR) or pathologically partial response (pPR), when remaining viable tumor was observed.

PET Imaging

Patients were scheduled for three PET studies: shortly before perfusion (median 14 days, range 1–30 days), 2 wk after perfusion (median 13 days, range 7–27 days) and shortly before resection of residual tumor tissue (median 55 days, range 42–77 days after perfusion). FDG was routinely produced by a robotic system following the procedure as described by Hamacher (*27*), with a radiochemical purity of more than 98%.

All patients fasted for at least 6 hr before the investigation. Serum glucose levels were measured before each PET session and were found to be normal. A 20-gauge needle was inserted into the radial artery under local anesthesia. In the contralateral arm, an intravenous canula was inserted in the cephalic vein for the injection of the FDG. The patients were positioned supine in the camera, with the tumor in the field of view based on physical examination.

After attenuation scanning using $^{68}Ge/^{68}Ga$ source, 370 MBq (10mCi) FDG were administered intravenously over 1 min. Dynamic images were acquired from the time of injection after a dynamic protocol (five 1-min, five 2-min, five 3-min, two 5-min, two 10-min, for a total duration of 60 min). Simultaneously, 2-ml blood samples were taken from the arterial canula (time points 0.5, 1, 1.5, 2, 2.5, 3, 3.5, 4, 4.5, 5, 10, 15, 25, 35, 45 and 55 min postinjection). The blood samples were centrifuged and plasma activity was assessed using a well counter that was cross-calibrated with the positron camera. Whole-body images were obtained after

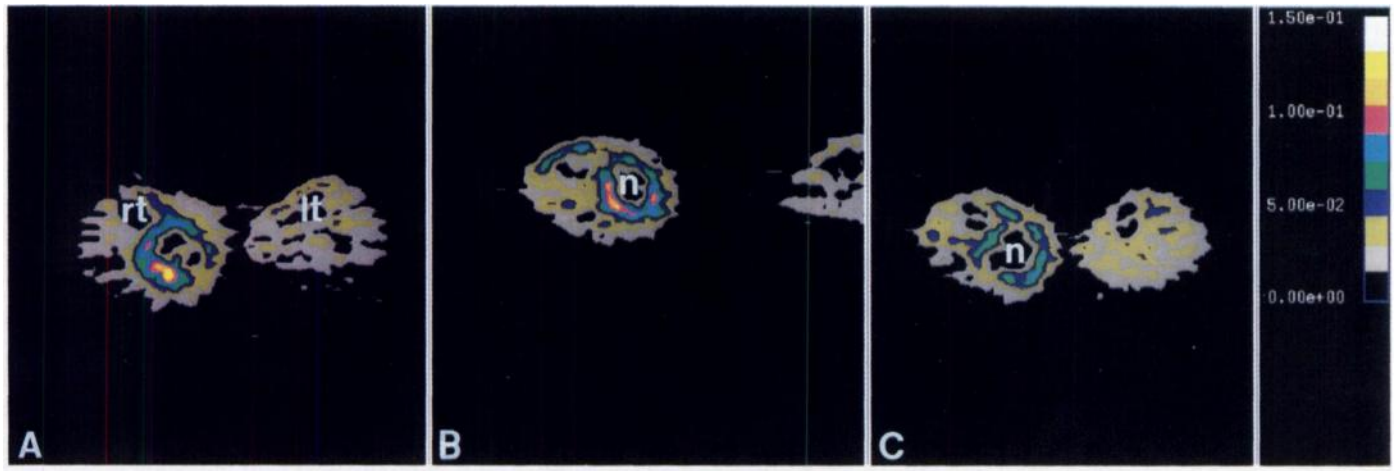

FIGURE 2. Transversal image of a malignant mixoid chondrosarcoma of the lower leg in Patient 8. Before perfusion (A), the tumor is clearly depicted as an inhomogeneous mass with a glucose uptake of 6.4 μmole/100 g tissue/min. Two (B) and 8 wk after perfusion (C), the glucose uptake in the tumor decreased to 4.6 and 3.9, respectively. Pathological examination revealed partial response. The rim signal corresponded with areas of viable tumor and inflammatory tissue surrounding a core of necrosis (n). The color scale equates a particular hue to a particular metabolic rate of glucose in mmol/100 g tissue/min (rt = right tibia; lt = left tibia).

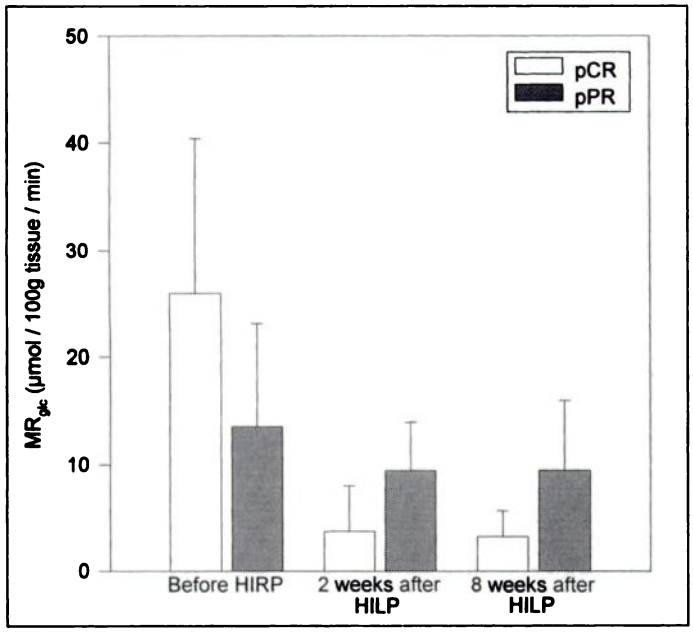

FIGURE 3. MR_{glc} of the tumor with s.d. before, 2 and 8 wk after perfusion. Before perfusion, the MR_{glc} in the pCR group was significantly higher than in the pPR group ($p < 0.05$). Two and 8 wk after perfusion, the MR_{glc} in the pCR group decreased significantly ($p < 0.05$) in contrast to the pPR group.

dynamic scanning. Total time for the imaging procedure was approximately 2.5 hr.

Data Analysis

Images were displayed in coronal, sagittal and transaxial projections on a computer display and interpreted independently by two experienced physicians. Before perfusion, the tumor location was first defined in all relevant tomographic planes of the study. Each tumor was outlined automatically with a threshold technique that defines its contours at a manually chosen percentage of the maximum number of counts per pixel. The level of the threshold was chosen with the purpose to match the size of the region of interest with the tumor size as outlined by MRI or CT. For each patient, a fixed percentage (mean 40, range 30–60) was used in all planes. All pixels above the threshold were used for the calculation.

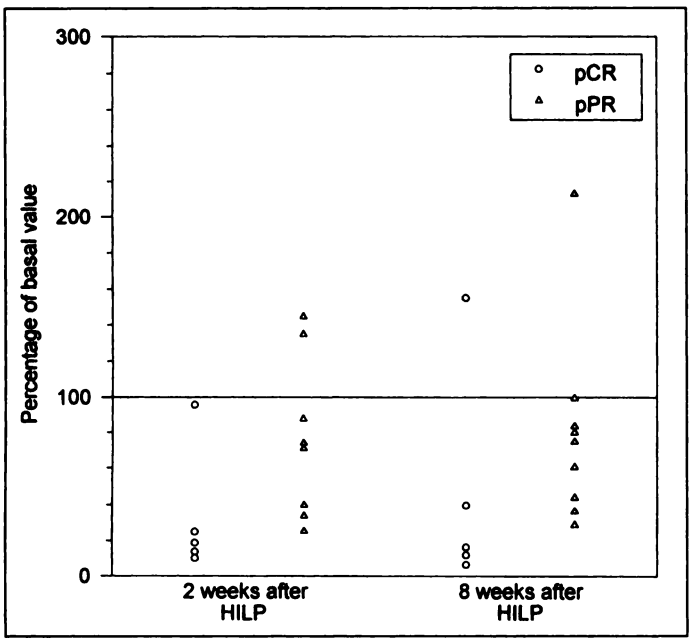

FIGURE 4. Percentage of basal value of the tumor for each patient 2 and 8 wk after perfusion.

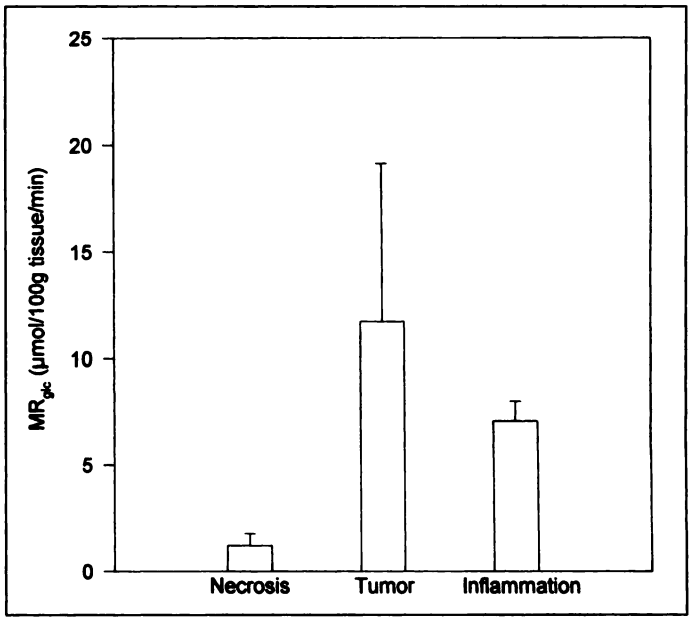

FIGURE 5. MR_{glc} in necrotic, tumor and inflammatory tissue. MR_{glc} in necrotic tissue was significantly lower ($p < 0.05$) than that in tumor and inflammatory tissue. The latter two could not be discriminated based on MR_{glc}.

An average time-activity curve as well as the total volume of the lesion was obtained. Combining the average time-activity data with the plasma input data, the average metabolic rate of glucose consumption (MR_{glc}) in µmole/100 g tumor tissue/min was calculated using Patlak analysis, assuming a lumped constant of 0.42 (*28,29*). After perfusion, this threshold technique could not be used since large areas of the tumors became inactive. The MR_{glc} after perfusion was therefore calculated by placing multiple regions of interest (ROI) over the original tumor in all relevant planes of the study. Consequently, the necrotic parts of the tumor that originated after perfusion were incorporated in this calculation. The MR_{glc} in the active parts of the tumor after perfusion was calculated separately with the ROI technique. The change in MR_{glc} after perfusion was related to the pre-perfusional value and expressed as a percentage of basal value.

Visual evaluation of the PET studies was performed by quantifying the degree of viable (active areas on the PET studies) and necrotic tumor (inactive areas) as a percentage before and after perfusion.

Statistical Analysis

Statistical procedures included a two-factor experiment with repeated measures on one factor to compare glucose consumption between measures and groups. Analyses were performed on datasets corrected for missing data according to Winer (*30*). Posthoc comparison was made with Student t-tests. A p value < 0.05 was considered significant.

RESULTS

The tumor characteristics, PET results and pathological response for each patient are summarized in Tables 1 and 2. Pathological examination of the residual tumor mass showed no viable tumor in seven patients (pCR 35%). In twelve patients, variable amounts of viable tumor were found (pPR 60%). The pPR group also included one patient with no change in the percentage of viable tumor after treatment (clinically this patient showed no response as well). In one patient (5%), the residual tumor was not excised because of progressive distant disease. This patient died 3 mo after perfusion and data from this patient are excluded from the remainder of the analyses. Forty-nine of the scheduled 60 PET studies were completed (82%).

Seven PET studies were not performed due to patient-related problems. Technical problems prevented quantification of PET data in four studies. Before perfusion, all tumors were easily visualized on the baseline FDG-PET images. Twelve patients showed homogeneous active tumor on the preperfusion PET study, whereas eight patients also showed inactive parts in the tumors before perfusion. Visual analysis of the PET images at 2 and 8 wk after perfusion showed a rim of increased FDG uptake around a core of absent FDG uptake in 12 patients (5 of 7 pCR, 7 of 12 pPR). The active rim corresponded in the pCR patients with a fibrotic vascular pseudocapsule with reactive inflammatory tissue, surrounding a core of absent FDG uptake representing necrosis (Fig. 1). In patients with pPR, the active rim was found to contain both viable tumor and an inflammatory response (Fig. 2). Thus, the rim signal could correspond with either viable tumor or a pseudocapsule with an inflammatory reaction. In seven patients, the tumor was visualized after perfusion as a homogeneous mass without the rim-core configuration (2 of 7 pCR, 5 of 12 pPR). After perfusion, the amount of active parts in the tumor declined significantly in 11 patients, corresponding with no or less than 20% viable tumor tissue in the pathological specimens in each of these patients. In two patients (Patients 3, 8) who also showed good pathological response, the PET study did not confirm this result. On histological examination, regressive tumor tissue with an inflammatory reaction was found in Patient 3 and areas of viable tumor accompanied by inflammatory tissue were found in Patient 8. The PET studies correctly indicated moderate pathological outcome in six patients. Overall, 17 of 19 responses were correctly indicated by FDG-PET (89%), but the discrimination between no and small amounts of viable tumor could not be made.

Pre-perfusion glucose consumption in the patients who ultimately had pCR was significantly higher ($p < 0.05$) than the pPR group (Fig. 3). At 2 and 8 wk postperfusion the MR_{glc} in the pCR group had decreased significantly ($p < 0.05$) in contrast to the MR_{glc} in the pPR group (Fig. 3). The most substantial decrease in MR_{glc} occurred within 2 wk after perfusion. Figure 4 shows the percentage of basal value of the tumor after perfusion. Patients in the pCR group showed a trend towards more reduced percentages of basal values than the pPR patients.

Three different histopathological groups could be distinguished after perfusion: necrotic tissue, represented by the core MR_{glc} of the pCR and pPR group, viable tumor in combination with an inflammatory response, represented by the rim MR_{glc} of the pPR group and inflammatory with pseudocapsular tissue, represented by the rim MR_{glc} of the pCR group. The average MR_{glc} in necrotic tissue was significantly lower ($p < 0.05$) than the values in tumor and inflammatory tissue, which were in the same range (Fig. 5).

DISCUSSION

PET has made it possible to study biochemical changes of cancer tissue and to study the effect of treatment on metabolism in vivo. The present study demonstrates substantial decrements in the glucose metabolism of soft-tissue sarcomas with pCR after perfusion with rTNF-α. These changes were already evident within 2 wk. In patients with a pPR, this decrease was less pronounced. An active rim with an inactive core was seen in 13 of 20 patients after perfusion. Pathological examination showed that areas of absent intratumoral FDG uptake were consistent with necrotic tissue. The rim signal represented either viable tumor or a fibrous pseudocapsule with inflammatory tissue. Unfortunately, FDG-PET could not discriminate a complete response from a partial response due to the overlap in glucose metabolism between viable tumor and inflammatory tissue.

An explanation for this rim-core pattern can be found in the working mechanism of TNF. Briefly, TNF exposure invokes an altered endothelial cell phenotype, anticoagulant mechanisms are suppressed and tissue factor is produced, which leads to fibrin accumulation at the endothelial cell surface and thrombus formation in the tumor vessels, causing circulatory stasis and ischemia inside the tumor followed by necrosis of the tumor cells adjacent to the occluded vessels (*31*). Necrotic tissue is unable to accumulate FDG and represents the core on the PET image. The central necrosis elicits an inflammatory response with the formation of a fibrous pseudocapsule. This is reflected by the rim on the PET image in the pCR group. On the other hand, peripheral tumor cells may obtain enough nutrients from the surrounding environment to survive. This is reflected by the rim signal in patients with pPR. Jones et al. (*32*) also found an active rim with FDG-PET after neo-adjuvant chemotherapy of soft-tissue sarcomas. In their patients, the rim signal did not signify viable tumor but only a fibrous pseudocapsule. FDG accumulation in active inflammatory lesions is in concordance with the observation of Tahara et al. (*33*) who found an increased glucose uptake in abdominal abscesses. Kubota et al. (*34*) also found a high accumulation in macrophages and granulation tissue in a microautoradiographic study. They state that one should consider not only the tumor cells as FDG uptake source but also the non-neoplastic cellular elements that may accompany tumor growth or necrosis. These phenomena will occur particularly in tumors subjected to treatment. The fact that both viable tumor and inflammatory tissue accumulate FDG is one of the major limitations of FDG as a radiopharmaceutical for cancer treatment evaluation.

One pCR patient showed an elevated MR_{glc} 8 wk after perfusion; in another pCR patient, the MR_{glc} did not decrease 2 wk after perfusion. These observations could be explained by the inflammatory cell invasion in the tumor. Besides the early vascular phenomenon, a subsequent immune effect with polymorphonuclear cell binding to the activated endothelium is another mechanism contributing to the anti-tumor effect of TNF (*35–37*). This homing of inflammatory cells in the tumor may be responsible for a high MR_{glc} after perfusion in these two patients. This is in concordance with the observation that FDG uptake was diffusely increased in the remainder of the perfused leg. This phenomenon is thought to be caused by the diffuse inflammatory reaction that follows perfusion.

Quantitative analysis demonstrated that the pre-perfusion MR_{glc} in the pCR group was significantly higher than in the pPR group. Thus, high MR_{glc} appears to predict good response to rTNF-α perfusion. Since glucose uptake in soft-tissue sarcoma correlates well with the malignancy grade of the tumor, high-grade tumors could be more susceptible to rTNF-α perfusion (*16,17*).

In 17 of 19 (89%) patients, visual evaluation of the PET studies corresponded well with the pathological response. In two patients with a good pathological response, the PET study did not confirm this. In these two patients, areas of inflammatory tissue were found on histological examination which corresponded with active areas on the PET scan and resulted in an overestimation of active tumor on the PET scans. Although visual evaluation gave a good indication of the pathological outcome, the use of FDG-PET in routine clinical monitoring of response of soft-tissue sarcomas to isolated limb perfusion is hampered by this overlap between malignant tumor and inflammatory tissue response.

Several other investigators have studied whether FDG-PET can be used to monitor treatment for cancer. FDG uptake was found to decrease as early as 5 days after the start of systemic

therapy for breast cancer (*20,38*). A change in FDG uptake was found to better predict the ultimate outcome than change in tumor size. Decreased FDG uptake was more prominent in patients who responded favorably to radiotherapy or chemotherapy for head and neck cancer compared to non-responding patients (*18,39*). Similar findings have been reported in other types of tumors and using a variety of therapeutic schedules (*19,40–43*). These studies have in common that post-treatment PET data were correlated with findings of physical examination, radiographic studies or, at best, fine needle aspiration of the tumor mass, following generally accepted guidelines (*44*). In none of these studies have the PET findings been verified by rigorous microscopic examination of the whole tumor as the gold standard as we have done in the present study. Our approach appears worthwhile, since changes in tumor volume and viability are not very well correlated. A palpable mass that remains after treatment may consist of necrosis and fibrosis without viable tumor. On the other hand, viable tumor may still remain when a palpable tumor that is visible on radiographic images disappears after treatment. If one wants to investigate whether PET signifies an improvement over radiographic techniques in the evaluation of treatment, it seems less appropriate to use those same radiographic techniques as the reference standard.

Our results should be interpreted with caution. Our patient population was limited in that it was a heterogeneous group of soft-tissue sarcomas and only large tumors were included (median 8.5 cm). Additional data are needed on FDG-PET in more patients with other tumor types treated with other drugs. Other PET tracers, such as labeled amino acids and ^{11}C-thymidine, may be more suitable for distinguishing between tumor and inflammatory response.

CONCLUSION

The present study demonstrated that FDG-PET indicates the pathologic tumor response to chemotherapy in an investigational setting used with isolated limb perfusion for locally advanced soft-tissue sarcomas. The discrimination between viable tumor and inflammatory tissue after perfusion treatment, however, was hampered by the limited specificity of FDG. A search for more specific tracers to monitor pathologic tumor response is needed.

REFERENCES

1. Mazanet R, Antman KH. Sarcomas of soft tissue and bone. *Cancer* 1991;68:463–473.
2. Suit HD. Local control and patient survival. *Int J Radiat Oncol Biol Phys* 1992;23:653–660.
3. Sadoski C, Suit HD, Rosenberg A, Mankin H, Efird J. Preoperative radiation, surgical margins and local control of extremity sarcomas of soft tissues. *J Surg Oncol* 1993;52:223–230.
4. Hoekstra HJ, Schraffordt Koops H, Molenaar WM, et al. A combination of intraarterial chemotherapy, preoperative and postoperative radiotherapy and surgery as limb-saving treatment of primarily unresectable high-grade soft tissue sarcomas of the extremities. *Cancer* 1989;63:59–62.
5. Eilber F, Eckardt J, Rosen G, Forscher C, Selch M. Improved complete response rate with neoadjuvant chemotherapy and radiation for high grade extremity soft-tissue sarcoma. *Proc Am Soc Clin Oncol* 1994;13:473.
6. Hoekstra HJ, Schraffordt Koops H, Molenaar WM, Oldhoff J. Results of isolated regional perfusion in the treatment of malignant soft-tissue tumors of the extremities. *Cancer* 1987;60:1703–1707.
7. Lehti PM, Moseley HS, Janoff K, Stevens K, Fletcher WS. Improved survival for soft-tissue sarcoma of the extremities by regional hyperthermic perfusion, local excision and radiation therapy. *Surg Gynecol Obstet* 1986;162:149–152.
8. Meyer M, Muchmore JH, Krementz ET. Pre- and perioperative perfusion chemotherapy for soft-tissue sarcoma of the limbs. *Cancer Treat Res* 1991;56:105–126.
9. Guchelaar HJ, Hoekstra HJ, De Vries EGE, Uges DR, Oosterhuis JW, Schraffordt Koops H. Cisplatin and platinum pharmacokinetics during hyperthermic isolated limb perfusion for human tumors of the extremities. *Br J Cancer* 1992;65:898–902.
10. Lienard D, Ewalenko P, Delmotte JJ, Renard N, Lejeune FJ. High-dose recombinant tumor necrosis factor alpha in combination with interferon gamma and melphalan in isolation perfusion of the limbs for melanoma and sarcoma. *J Clin Oncol* 1992;10:52–60.
11. Eggermont AMM, Lienard D, Schraffordt Koops H, Rosenkaimer F, Lejeune FJ. Treatment of irresectable soft-tissue sarcomas of the limbs by isolation perfusion with high dose TNFalfa in combination with interferon-gamma and melphalan. In: Fiers W, Buurman WA, eds. *Tumor necrosis factor: molecular and cellular biology and clinical relevance*. 1st ed. Basel: Karger; 1993:239–243.
12. Strauss LG, Conti PS. The applications of PET in clinical oncology. *J Nucl Med* 1991;32:623–648.
13. Kern KA, Brunetti A, Norton JA, et al. Metabolic imaging of human extremity musculoskeletal tumors by PET. *J Nucl Med* 1988;29:181–186.
14. Warburg O. On the origin of cancer cells. *Science* 1956;123:309–314.
15. Griffeth LK, Dehdashti F, McGuire AH, et al. PET evaluation of soft-tissue masses with fluorine-18 fluoro-2-deoxy-D-glucose. *Radiology* 1992;182:185–194.
16. Adler LP, Blair HF, Makley JT, et al. Noninvasive grading of musculoskeletal tumors using PET. *J Nucl Med* 1991;32:1508–1512.
17. Nieweg OE, Pruim J, van Ginkel RJ, et al. Fluorine-18-fluorodeoxyglucose PET imaging of soft-tissue sarcoma. *J Nucl Med* 1996;37:257–261.
18. Minn H, Paul R, Ahonen A. Evaluation of treatment response to radiotherapy in head and neck cancer with fluorine-18-fluorodeoxyglucose. *J Nucl Med* 1988;29:1521–1525.
19. Ichiya Y, Kuwabara Y, Otsuka M, et al. Assessment of response to cancer therapy using fluorine-18-fluorodeoxyglucose and positron emission tomography. *J Nucl Med* 1991;32:1655–1660.
20. Wahl RL, Zasadny K, Helvie M, Hutchins GD, Weber B, Cody R. Metabolic monitoring of breast cancer chemohormonotherapy using positron emission tomography: initial evaluation. *J Clin Oncol* 1993;11:2101–2111.
21. Enzinger FM, Weiss SW. *Soft-tissue tumors*. St Louis: Mosby; 1988.
22. Coindre JM, Trojani M, Contesso G, et al. Reproducibility of a histopathologic grading system for adult soft-tissue sarcoma. *Cancer* 1986;58:306–309.
23. Creech O, Krementz ET, Ryan RF, Winblad JN. Chemotherapy of cancer: regional perfusion utilizing an extracorporeal circuit. *Ann Surg* 1958;148:616–632.
24. Fontijne WP, Mook PH, Schraffordt Koops H, Oldhoff J, Wildevuur CR. Improved tissue perfusion during pressure regulated regional perfusion: a clinical study. *Cancer* 1985;55:1455–1461.
25. Wieberdink J, Benckhuysen C, Braat RP, Van Slooten EA, Olthuis GAA. Dosimetry in isolation perfusion of the limb by assessment of perfused tissue volume and grading of toxic tissue reactions. *Eur J Cancer Clin Oncol* 1982;18:905–910.
26. Schraffordt Koops H. Prevention of neural and muscular lesions during hyperthermic regional perfusion. *Surg Gynecol Obstet* 1972;135:401–403.
27. Hamacher K, Coenen HH, Stöcklin G. Efficient stereospecific synthesis of no-carrier-added ^{18}F-fluoro-2-deoxy-D-glucose using aminopolyether supported nucleophilic substitution. *J Nucl Med* 1986;27:235–238.
28. Patlak CS, Blasberg RG, Fenstermacher JD. Graphical evaluation of blood-to-brain transfer constants from multiple-time uptake data. *J Cereb Blood Flow Metab* 1983;3:1–7.
29. Patlak CS, Blasberg RG. Graphical evaluation of blood-to-brain transfer constants from multiple-time uptake data. Generalizations. *J Cereb Blood Flow Metab* 1985;5:584–590.
30. Winer BJ. *Statistical principles in experimental design*. New York: McGraw Hill; 1971.
31. Nawroth P, Handley D, Matsueda G, de Waal R, Gerlach H, Blohm DSD. Tumor necrosis factor/cachectin-induced intravascular fibrin formation in meth A fibrosarcomas. *J Exp Med* 1988;168:637–647.
32. Jones DN, Brizel DM, Charles HC, et al. Monitoring of response to neoadjuvant therapy of soft tissue and musculoskeletal sarcomas using ^{18}F-FDG PET [Abstract]. *J Nucl Med* 1994;35(suppl):38P.
33. Tahara T, Ichiya Y, Kuwabara Y, Otsuka M, Miyake Y, Gunasekera RMK. High [^{18}F]fluorodeoxyglucose uptake in abdominal abscesses: a PET study. *J Comput Assist Tomogr* 1989;13:829–831.
34. Kubota R, Yamada S, Kubota K, Ishiwata K, Tamahashi N, Ido T. Intratumoral distribution of fluorine-18-fluorodeoxyglucose in vivo: high accumulation in macrophages and granulation tissues studied by microautoradiography. *J Nucl Med* 1992;33:1972–1980.
35. Palladino MA Jr, Shalaby MR, Kramer SM, et al. Characterization of the antitumor activities of human tumor necrosis factor-α and the comparison with other cytokines: induction of tumor-specific immunity. *J Immunol* 1987;138:4023–4032.
36. Gamble JR, Harlan JM, Klebanoff SJ, Vadas MA. Stimulation of the adherence of neutrophils to umbilical vein endothelium by human recombinant tumor necrosis factor. *Proc Natl Acad Sci USA* 1985;82:8667–8671.
37. Renard N, Lienard D, Lespagnard L, Eggermont AMM, Heimann R, Lejeune FJ. Early endothelium activation and polymorphonuclear cell invasion precede specific necrosis of human melanoma and sarcoma treated by intravascular high-dose tumor necrosis factor alpha (rTNFα). *Int J Cancer* 1994;57:656–663.
38. Nieweg OE, Wong WH, Singletary SE, Hortobagyi GN, Kim EE. Positron emission tomography of glucose metabolism in breast cancer. Potential for tumor detection, staging and evaluation of chemotherapy. *Ann NY Acad Sci* 1993;698:423–428.
39. Haberkorn U; Strauss LG, Dimitrakopoulou A, et al. Fluorodeoxyglucose imaging of advanced head and neck cancer after chemotherapy. *J Nucl Med* 1993;34:12–17.
40. Haberkorn U, Strauss LG, Dimitrakopoulou A, et al. PET studies of fluorodeoxyglucose metabolism in patients with recurrent colorectal tumors receiving radiotherapy. *J Nucl Med* 1991;32:1485–1490.
41. Strauss LG, Dimitrakopoulou A, Haberkorn U, Ostertag H, Helus F, Lorenz WJ. PET studies with FDG in patients with metastatic melanoma prior and after therapy. *Eur J Nucl Med* 1991;18:685.
42. Abe Y, Matsuzawa T, Fujiwara T, et al. Clinical assessment of therapeutic effects on cancer using ^{18}F-2-fluoro-2-deoxy-D-glucose and positron emission tomography: preliminary study of lung cancer. *Int J Radiat Oncol Biol Phys* 1990;19:1005–1010.
43. Bares R, Horstmann K, Altehoefer C, et al. FDG-PET to assess local effects of radiation or chemotherapy in patients with malignant lymphoma [Abstract]. *J Nucl Med* 1991;32(suppl):918P.
44. Miller AB, Hoogstraten B, Staquet M, Winkler A. Reporting results of cancer treatment. *Cancer* 1981;47:207–214.